JOURNAL OF CATALYSIS **166,** 244–253 (1997)
ARTICLE NO. CA971519

Partial Oxidation of Methane on Supported Potassium Molybdate

A. Erdőhelyi, K. Fodor, and F. Solymosi

Institute of Solid State and Radiochemistry, A. József University and Reaction Kinetics Research Group of the Hungarian Academy of Sciences, P.O. Box 168, H-6701 Szeged, Hungary[1]

Received April 26, 1996; revised September 20, 1996; accepted October 31, 1996

The partial oxidation of methane to formaldehyde was studied on K_2MoO_4, deposited on various supports, in a fixed-bed continuous-flow reactor at 860–923 K using O_2 as oxidant. The catalysts were characterized by Raman and XPS spectroscopies. It was found that the composition of molybdates deposited by impregnation depended sensitively on the pH value of the slurry containing the support. At low pH values a significant amount of $K_2Mo_2O_7$ was formed. The product distribution of the oxidation reaction was markedly influenced by the nature of the support. The highest activity was measured for magnesia-supported catalyst. In this case, however, only the complete oxidation of methane occurred. Formaldehyde, in a larger quantity, was produced on silica-supported catalyst containing a greater amount of $K_2Mo_2O_7$ and on K_2MoO_4/ZSM-5. It was observed that at very low oxygen content, ~0.1%, the reaction pathway of methane conversion was basically different: in this case the main hydrocarbon products were ethylene, ethane, and benzene. Formaldehyde was not detected. A possible mechanism for the reaction of methane is discussed.

1. INTRODUCTION

The catalytic oxidation of methane into more valuable compounds, such as ethane, ethylene, formaldehyde, or methanol, is a focus of interest in both industrial and fundamental catalysis. Silica-supported molybdenum oxide was found to be one of the most active and selective catalysts for the partial oxidation of methane with O_2 (1–18) and with N_2O (19–21). When oxygen was used as an oxidant, formaldehyde was obtained as the main partial oxidation product over silica-supported MoO_3 catalysts (3–18). Selectivities to HCHO between 30 and 89% were observed at 5.0–0.01% methane conversion (3). MoO_3/SiO_2 also catalyzed the $CH_4 + N_2O$ reaction (steam is present in the system) to methanol and formaldehyde (19–21). At a conversion level of 3%, the selectivity to CH_3OH and HCHO was 14 and 64%, respectively (19).

Recently, it was reported that supported Mo oxides (22–26) are active catalysts in the high-temperature (~973 K) conversion of methane into benzene with 60–80% selectivity under nonoxidative conditions. Supported MoO_3 catalyst was found to be active in the oxidative dehydrogenation of ethane to give ethylene and acetaldehyde (27). In this case the addition of various compounds of potassium to MoO_3/SiO_2 greatly enhanced the conversion of ethane and increased the selectivity to acetaldehyde (28). However, the best catalytic performance was obtained when K_2MoO_4 was used as catalyst (28, 29). Similar features were observed for V_2O_5/SiO_2 promoted by alkali compounds and for KVO_3 catalyst (30, 31).

The catalytic performance of alkali metal molybdates in the partial oxidation of CH_4 has not yet been much explored. However, in the oxidative coupling of CH_4 they have been reported to exhibit good catalytic activity (31). K_2MoO_4/ZSM-5 was also found to be active in the conversion of methane into benzene under nonoxidative conversion (25).

The present paper gives an account of the selective oxidation of methane with O_2 on K_2MoO_4 catalysts using different supports. Attention is paid to the effects of the catalyst preparation on the structure of the catalysts and on the product distribution of the reaction.

2. EXPERIMENTAL

Materials. The catalysts were prepared by impregnating the supports with a basic solution (pH 11.0) of potassium molybdate (K_2MoO_4 (Aldrich)) to yield a nominal 2% loading of MoO_3 by weight (28). The following oxides were used as support: SiO_2 (Cab-O-Sil, 200 m^2/g), Al_2O_3 (Degussa P110 C1, 100 m^2/g), TiO_2 (Degussa P25, 150 m^2/g), MgO (DAB 6, 170 m^2/g), and H-ZSM-5 (Si/Al = 55.0, 350 m^2/g). During the impregnation we observed a decrease in the pH value, which was the largest for silica. In this case the pH value of the slurry was restored to pH 11. This sample is denoted as K_2MoO_4/SiO_2(II). The suspension was dried at 373 K and calcined at 863 K for 5 h.

Before any measurements, the catalysts were oxidized in an O_2 stream at 773 K *in situ* then flushed with He and heated to the reaction temperature in flowing He.

[1] This laboratory is a part of the Center for Catalysis, Surface and Material Science at the University of Szeged.

0021-9517/97 $25.00

The reactant gases, CH_4 (99.995%) and O_2 (99.99%), were used as received. He (99.996%) was purified with an oxy-trap.

Methods. The reactions were carried out in a fixed-bed continuous-flow reactor made of quartz (100 × 27 mm o.d.). Generally 0.5 g of sample was used as catalyst. The dead volume of the reactor was filled with quartz beads. The reacting gas mixture usually consisted of 90% CH_4 and 10% O_2. The flow rate of reactants was 50 ml/min and the space velocity was 6000 h^{-1}.

The gases were analyzed gas chromatographically (Chrompack 9001) by thermal conductivity and flame ionization detectors. A Porapak QS column was used to analyze CH_4, CO_2, C_2H_6, C_2H_4, HCHO, and CH_3OH. The separation of O_2 and CO was accomplished with a Carboxen 1000 column (Supelco) (1/8″ × 15′). The formaldehyde standard for the calibration curves was prepared by dissolving paraformaldehyde and was analyzed by Romijn's iodometric titration method (33).

The conversion and the selectivity for reaction products, S_i, were defined as

$$\text{Conversion} = \frac{\sum x_i n_i}{x_{CH_4} + \sum x_i n_i}$$

and

$$\text{Selectivity } S_i = \frac{x_i n_i}{\sum x_i n_i},$$

where x_i and x_{CH_4} are the mole fraction of product (i) and CH_4, respectively, and n_i is the number of carbon atoms in each molecule of product (i).

Raman spectra were recorded by a Bio-Rad FT-Raman spectrometer, which possessed a Spectra-Physics T 10-106 c Nd : YVO_4 laser. It was tuned to the exciting line at 1064 nm. The radiation intensity was varied from 540 to 1200 mW. A liquid nitrogen cooled Ge detector was used. In the case of supported samples 4096 scans, in other cases 128 scans, resulted in a sufficient signal-to-noise ratio. For elaboration and for subtraction of the spectra of the support, WIN-IR (Grams/386 Based Galactic Industries) software was used.

XPS measurements were preformed in a Kratos XSAM 800 instrument at a base pressure of 10^{-8} Torr using Mg$K\alpha$ (1253.6 eV) primary radiation (14 kV, 15 mA) (24, 25). To compensate for a possible charging effect, binding energies were normalized with respect to the position of the C(1s), this value being assumed constant at 285.1 eV. The pass energy was set at 40 eV; an energy step of 50 meV and dwell time of 300 ms were used. Typically 10 scans were accumulated for each spectrum. Fitting and deconvolution of the spectra were made using the VISION software (Kratos).

The number of basic sites was determined by adsorption of CO_2 at room temperature by dosing the sample with CO_2 pulses (5.2 μmol). The number of acidic sites was measured by n-butylamine titration. Data are collected in Table 1.

TABLE 1

Some XPS and Other Characteristic Data of Supported K_2MoO_4

	BE of Mo 3d		BE of K	Peak area	Acidic sites
	$3d_{5/2}$ (eV)	$3d_{3/2}$ (eV)	$2p_{3/2}$ (eV)	ratio[a]	(μmol/g)
MoO_3	233.0	236.2			
K_2MoO_4	232.0	235.2	292.5		
MoO_3/SiO_2 (24)	232.1	235.3		2.01	
K_2MoO_4/SiO_2	232.3	235.3	293.0	0.76	235.5
K_2MoO_4/SiO_2(II)	232.4	235.4	293.4	1	211.6
K_2MoO_4/Al_2O_3	232.8	235.8	293.3	5.34	147.1
K_2MoO_4/TiO_2	232.3	235.5	292.8	9.9	67.6
K_2MoO_4/ZSM-5	232.4	235.4	293.2	6.0	550.0
K_2MoO_4/MgO	232.6	235.7	293.1	1.69	—

[a] Area ratio of Mo 3d doublet for different supported K_2MoO_4 and MoO_3/SiO_2 taking as unit the area of K_2MoO_4/SiO_2.

3. RESULTS

3.1. Characterization of Catalysts

XPS spectra. The photoelectron spectra of the samples showed the characteristic Mo 3d doublet. The binding energy of the Mo $3d_{5/2}$ in MoO_3 is significantly higher (233.0 eV) than in K_2MoO_4 (232.0 eV).

The binding energy of Mo $3d_{5/2}$ for silica-supported K_2MoO_4 was somewhat higher (232.3–232.4 eV) than for the unsupported compound, but the FWHM was almost the same. Similar values were obtained for TiO_2- and ZSM-5-supported K_2MoO_4. In the case of K_2MoO_4/Al_2O_3 and K_2MoO_4/MgO, the binding energy of the Mo $3d_{5/2}$ was 232.8 eV and 232.6 eV, respectively (Fig. 1).

Interestingly, we found significantly lower values in the binding energies of the K 2p doublet (292.5 eV) for K_2MoO_4 than for different supported K_2MoO_4 samples (293.4–292.8 eV). Some characteristic XPS data are collected in Table 1.

Raman spectra. Raman spectra of supported and unsupported K_2MoO_4 samples are displayed in Fig. 2. For comparison the Raman spectrum of MoO_3 is also shown. The Raman frequencies of unsupported K_2MoO_4 (888, 852, 822, and 317 cm^{-1}) and those of MoO_3 (995, 819, 666, 379, 337, 290, 244, 217, 147, 157, 128, and 115 cm^{-1}) agree very well with those reported earlier (34, 35).

When K_2MoO_4 was supported on SiO_2 new weak bands at 931 and 908 cm^{-1} appeared in the Raman spectrum which were not observed in the spectrum of unsupported K_2MoO_4 (Fig. 2). The intensities of these peaks were much less pronounced for K_2MoO_4/SiO_2(II). The development of the peak at 931 and 908 cm^{-1} suggests the formation of a new compound on the silica surface, very probably $K_2Mo_2O_7$. Its characteristic frequencies are 930, 908, 873, and 860 cm^{-1} (36). The Raman spectra of other supported

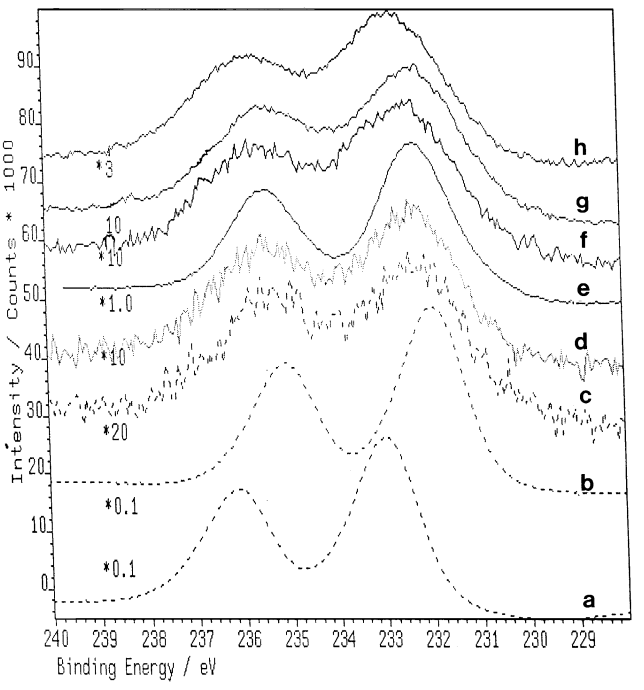

FIG. 1. XP spectra of MoO_3 (a); K_2MoO_4 (b); K_2MoO_4/SiO_2(II) (c); K_2MoO_4/SiO_2 (d); K_2MoO_4/TiO_2 (e); K_2MoO_4/MgO (f); K_2MoO_4/ZSM-5 (g); K_2MoO_4/Al_2O_3 (h).

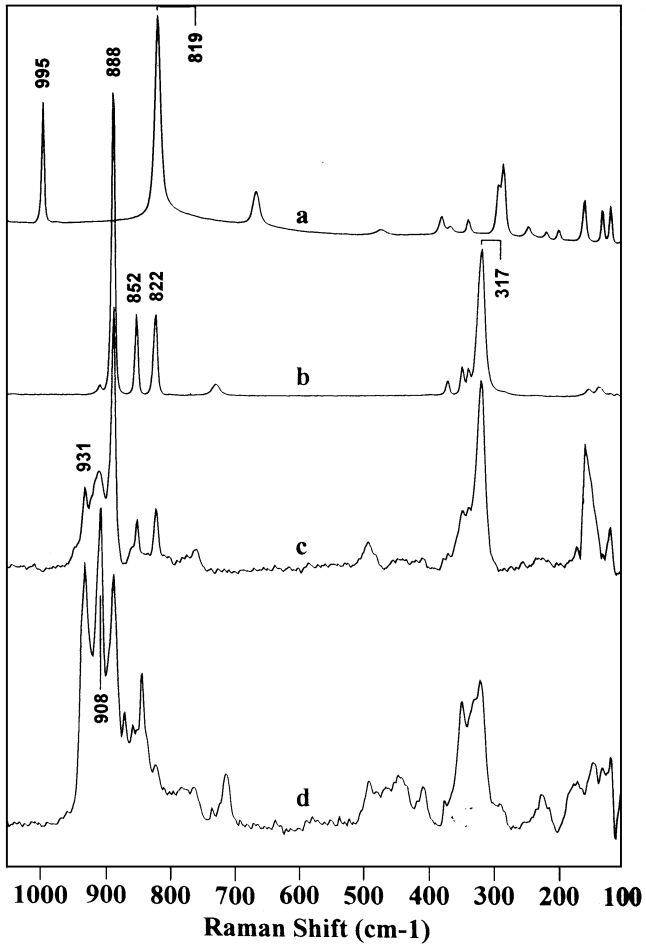

FIG. 2. Laser Raman spectra of (a) MoO_3, (b) K_2MoO_4, (c) K_2MoO_4/SiO_2(II), and (d) K_2MoO_4/SiO_2 catalysts.

K_2MoO_4 samples could not be analyzed because of the high sample fluorescence (Al_2O_3, ZSM-5) or because of the very weak signals detected (TiO_2, MgO). When the K_2MoO_4 content of the TiO_2-supported samples was increased to 5 or 10%, the Raman shifts characteristic of the K_2MoO_4 appeared in the spectra. In the case of K_2MoO_4/MgO, however, peaks were not detected even at higher molybdate concentration. The positions of the main Raman shifts and their possible assignments are shown in Table 2.

3.2. Oxidation of Methane on Supported K_2MoO_4 Catalysts

The first part of our studies was concerned with the catalytic effect of silica-supported samples. The reaction was carried out at 923 K and the inlet gas contained 90% CH_4 and 10% O_2. Figures 3 and 4 show the rates and selectivities of the formation of various products for the two K_2MoO_4 samples. The products of the reaction were formaldehyde, ethane, carbon monoxide, carbon dioxide, and water. Traces of methanol and ethylene were also detected. A significant decay in the rate of product formation occurred during the conditioning period at 923 K. The initial conversion of methane on K_2MoO_4/SiO_2 was about 3.3–3.5% which decreased to 1.2–1.3% after 200 min. At the same time the oxygen conversion decreased from 35.6 to 9%. The activity of the catalyst could be restored by oxidation neither at 773 K nor at 823 K even in the presence of water vapor. On the K_2MoO_4/SiO_2(II) sample the main product of the total oxidation was CO; the selectivity for HCHO formation was 20%. On K_2MoO_4/SiO_2, CO_2 was the dominant product. In this case the HCHO formation rate was about twice as high as on the previous sample. The selectivity to HCHO was also higher, ~30%.

Similar features were observed for other supported catalysts. The conversion of methane and selectivities to

TABLE 2

Raman Frequencies of MoO_3 and Potassium Molybdates

Sample	ν_s (Mo–O) (cm^{-1})	ν_a (Mo–O) (cm^{-1})	δ (Mo–O) (cm^{-1})	Ref.
MoO_3	995	819		This work
K_2MoO_4	888	852	317	This work
	886	848	313	(34)
$K_2Mo_2O_7$	929 (Oct.), 908 (Tet.)	873 (Oct.), 860 (Tet.)		(36)
K_2MoO_4/SiO_2(II)	888	852	317	This work
K_2MoO_4/SiO_2	931, 908, 881	873, 860, 852		This work
K_2MoO_4/TiO_2	888	840	314	This work

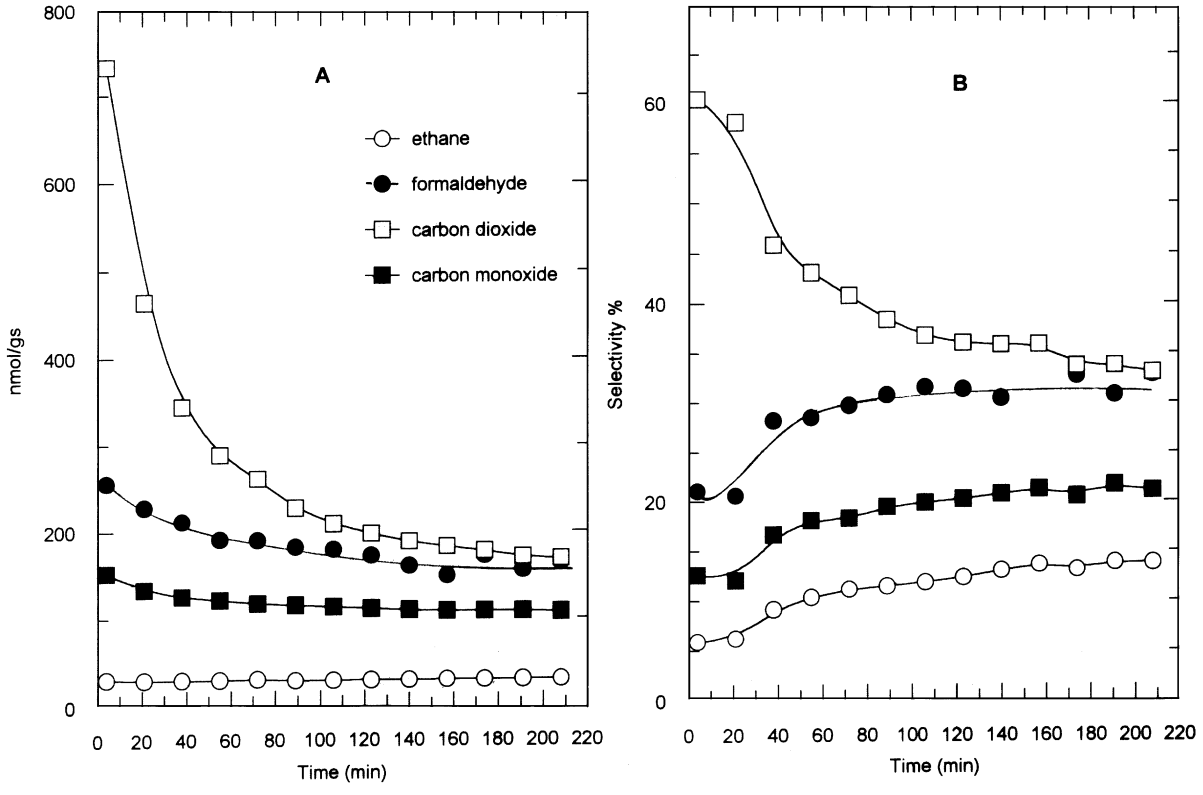

FIG. 3. (A) Rate and (B) selectivity of the formation of various products in the oxidation of CH_4 on K_2MoO_4/SiO_2 at 923 K.

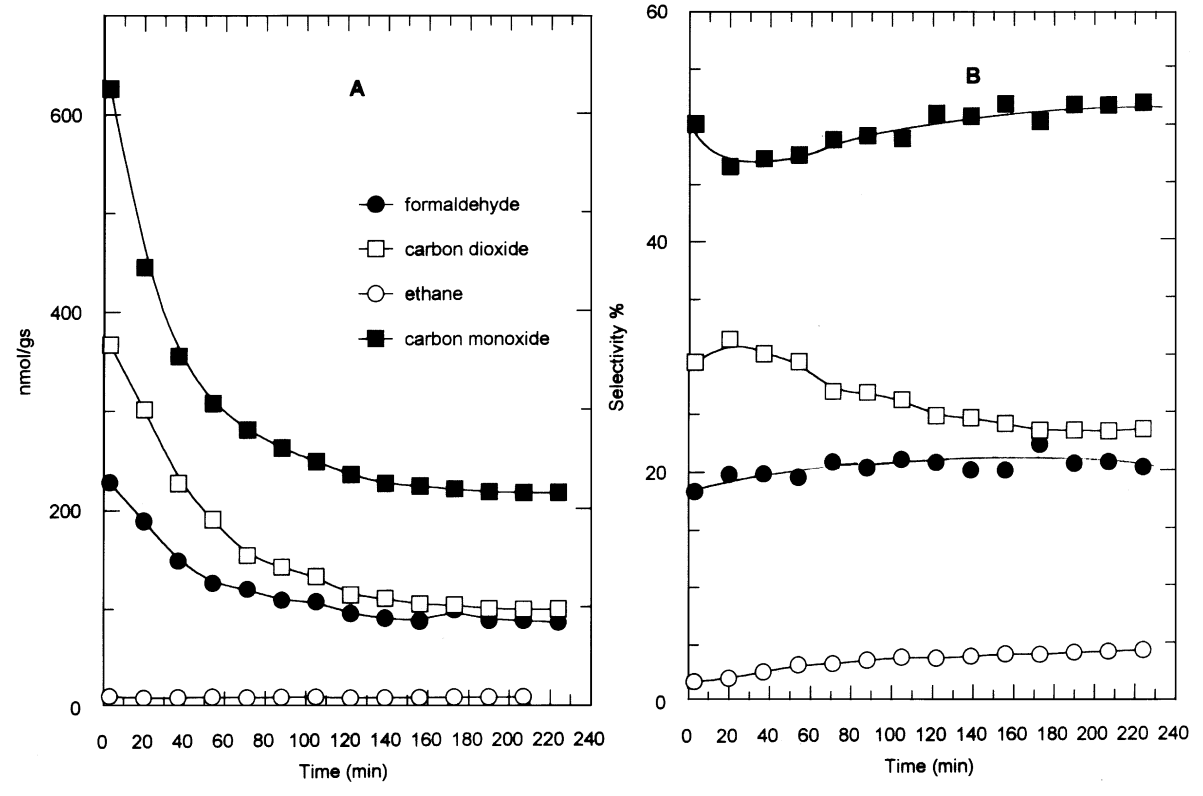

FIG. 4. (A) Rate and (B) selectivity of the formation of various products in the oxidation of CH_4 on K_2MoO_4/SiO_2(II) at 923 K.

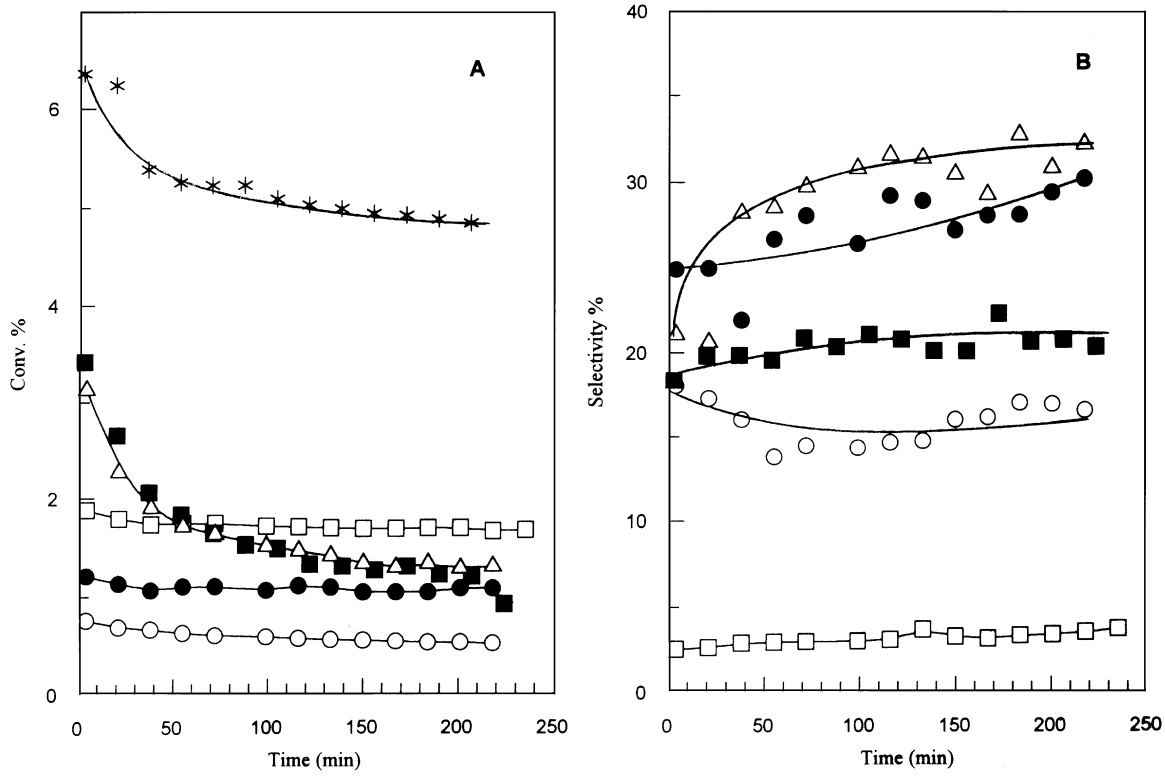

FIG. 5. (A) Conversion of CH_4 and (B) selectivity to HCHO at 923 K on (■) K_2MoO_4/SiO_2(II), (△) K_2MoO_4/SiO_2, (□) K_2MoO_4/Al_2O_3, (●) K_2MoO_4/ZSM-5, (○) K_2MoO_4/TiO_2, and (∗) K_2MoO_4/MgO.

HCHO and CO_2 are shown in Fig. 5. The selectivities for HCHO formation were the highest on K_2MoO_4/SiO_2 and K_2MoO_4/ZSM-5. On K_2MoO_4/Al_2O_3 catalysts only traces of HCHO were detected. No HCHO was identified for K_2MoO_4/MgO, where the complete oxidation of CH_4 was the dominant process. Some characteristic data are given in Table 3.

The effects of the different experimental conditions on the product distribution were determined on K_2MoO_4/SiO_2 pretreated with reacting gas mixture at 923 K until a steady-state activity was reached. The variation of space velocity exerted divergent influences on the characteristics of the methane oxidation. The conversion of methane and the rates of product formation linearly increased with the rise of the contact time. While the selectivity of carbon dioxide continuously increased with increasing the contact time, the CO selectivity curve exhibited a maximum. The selectivity to HCHO formation decreased up to the maximum of CO selectivity (Fig. 6A).

The temperature dependence of the reaction was studied in the range 860–923 K. At the steady state the selectivity of formaldehyde formation increased and that of C_2 hydrocarbon formation slightly decreased with decreasing the temperature; at 860 K these values were about 50

TABLE 3

Some Characteristic Data for CH_4 Oxidation ($CH_4/O_2 = 9$) at 923 K on Supported K_2MoO_4 Catalysts

		Rate of product formation (nmol/g · s)				Selectivity of product formation (%)			
	CH_4 conv. (%)	HCHO	CO	CO_2	C_2	HCHO	CO	CO_2	C_2
K_2MoO_4/SiO_2(II)	1.2	86	216	96	8.8	20.7	51.6	23.3	4.3
K_2MoO_4/SiO_2	1.3	163.5	107	168	35.0	32.1	21.0	32.9	13.7
K_2MoO_4/Al_2O_3	1.67	26	434	208	16.4	3.7	61.3	29.8	4.6
K_2MoO_4/TiO_2	0.53	36.8	41	123	7.8	16.9	18.8	56.6	7.3
K_2MoO_4/ZSM-5	1.07	135	188	113	5.7	30.1	42.0	25.2	1.2
K_2MoO_4/MgO	4.84	—	430	1926.5	11.0	—	18.0	81.0	0.93

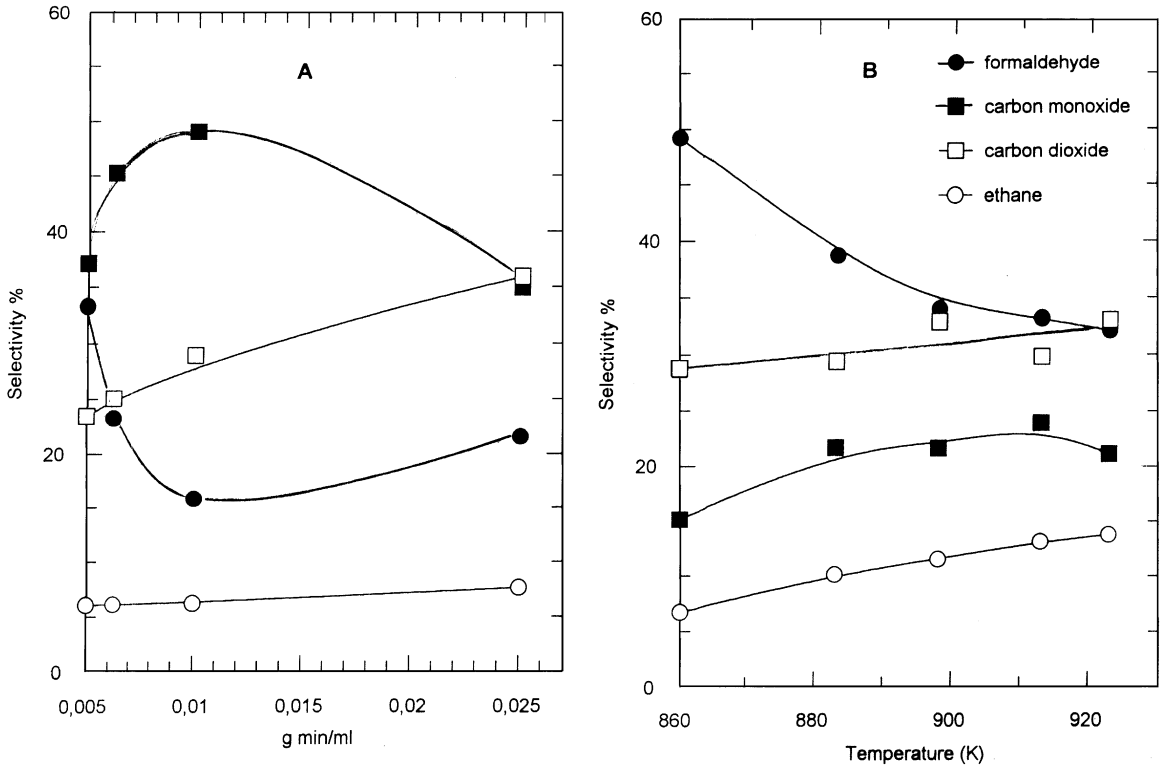

FIG. 6. The selectivity of product formation as a function of (A) the contact time at 923 K and (B) temperature on K_2MoO_4/SiO_2. The concentrations of CH_4 and O_2 were 90 and 10%, respectively.

and 5%, respectively (Fig. 6B). The temperature dependence of the rates of HCHO, CO, and CO_2 formation gives good Arrhenius fits within the limits of experimental uncertainty. The apparent activation energies for the formation of these compounds were 110, 187, and 166 kJ/mol, respectively. Nearly the same activation energies were calculated for the formation of these compounds on K_2MoO_4/SiO_2(II) catalyst.

Regarding the effects of the concentration of reactants, we found that increasing the O_2 concentration (6–30%) the conversion of methane and the rates of formation of products increased. The selectivity for HCHO and CO_2 formation decreased, whereas that of CO significantly increased. An increase in the methane content of the reacting gas mixture (66–90%) also enhanced the rates of product formation. The selectivities, however, changed only slightly.

The kinetic order with respect to O_2 was found to be about 0.5 up to 20% of oxidant for HCHO (0.6) and CO_2 (0.45) formation. It was higher (1.2) for CO production. Above this concentration range the rate of formation of products suddenly increased. The order with respect to methane is about 0.5 for HCHO and C_2H_6 formation at 65–85% of CH_4 content. It was 1.77 for CO and 0.82 for CO_2 formation. At higher CH_4 content (~90%) the rate of formation of products drastically increased.

3.3. Conversion of Methane at Very Low Oxygen Concentration

In the subsequent measurements the reaction of methane was followed at very low oxygen content. Recently we found that under nonoxidative conditions the reaction of methane on K_2MoO_4/ZSM-5 yields completely different products: ethylene, ethane, and benzene (25). It was interesting to see how the partial pressure of oxygen influences the reaction pathways of methane. Experiments were performed at 973 K. The space velocity was the same as used earlier in this study. Results obtained are presented in Fig. 7. In the absence of oxygen we observed the same behavior as experienced before (25). At the beginning, H_2O, CO, and CO_2 were formed suggesting that methane reacted with the catalyst. After the cessation of the production of these compounds, the formation of benzene came into prominence together with ethylene and ethane (Figs. 7A and 7B). The selectivity to benzene was 38–48%. (Note that at lower space velocity we measured a value of 60–65% (25)). Interestingly, H_2 was produced at the very beginning of the reaction; its amount, after a sharp maximum, gradually decreased with time on stream (Fig. 7C). The CH_4 conversion varied between 0.8 and 0.3%.

Adding 0.1% of O_2 to the CH_4, the conversion of methane slightly decayed (Fig. 7D). The main C-containing

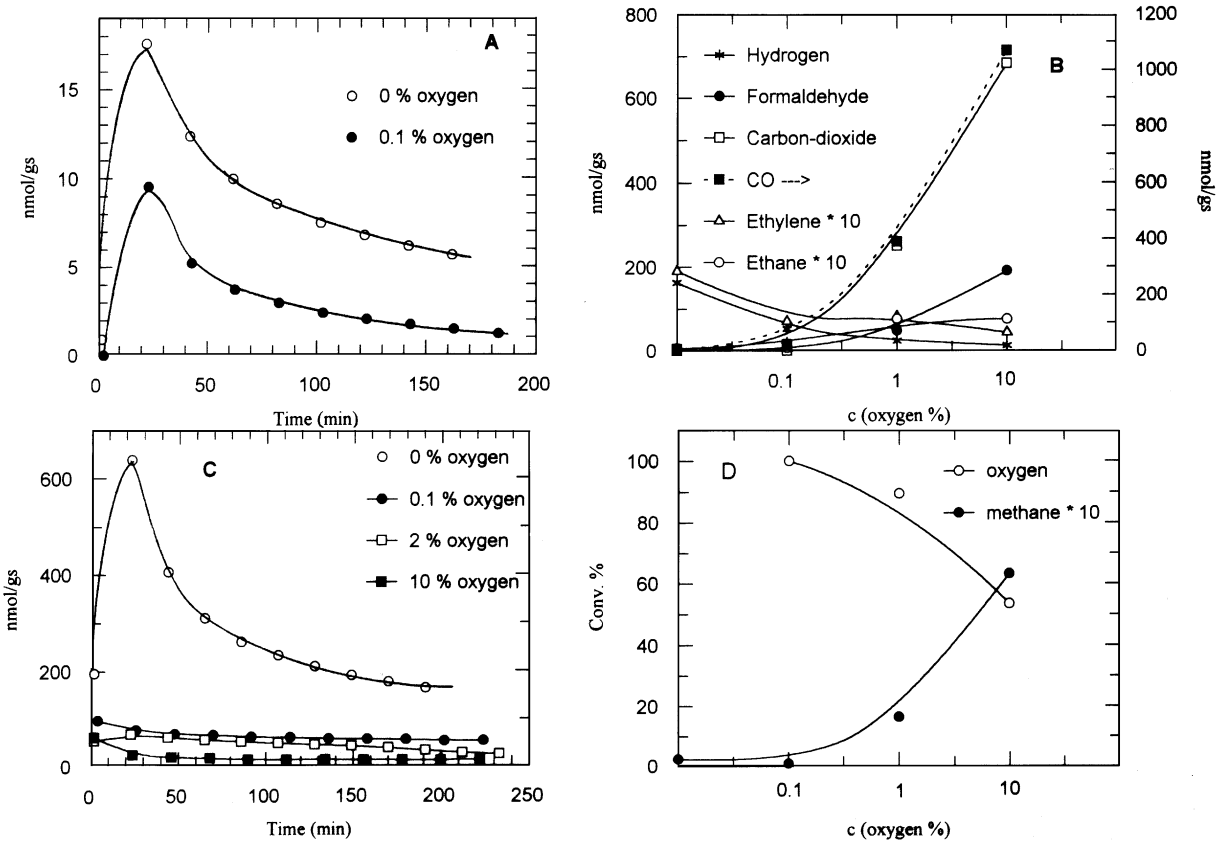

FIG. 7. Rate of formation of (A) benzene and (C) H_2 with time on stream. (B) Rate of product formation and (D) the conversion of methane at the steady state as a function of O_2 concentration. The reaction temperature was 973 K. The concentration of CH_4 was 90% and He was used as diluent gas.

products were CO ($S = 30$–50%), C_2H_4 ($S = 21$–35%), benzene ($S = 43$–15%), and ethane ($S = 3.6$–1.7%).

Further increasing the O_2 content to 1%, the conversion of methane was drastically enhanced by a factor of 8 (Fig. 7D). In addition to the compounds of total oxidation, formaldehyde appeared in the products ($S = 6$–8%) (Fig. 7B), but benzene was no longer detected. Ethylene ($S = 2.0$–2.5%) and ethane ($S = 1.5$–2.0%) were also formed. At 10% of O_2 content we observed the same features as mentioned before. The selectivity to formaldehyde was somewhat lower than that obtained at 923 K. The amount of C_2 compounds was the highest in this case.

3.4. Examination of the Used Catalyst

In order to establish changes on the catalyst surface the reaction was interrupted at different stages and the catalysts were examined. After 1 h of reaction we found only a trace amount of carbon on the K_2MoO_4/SiO_2 (<0.1 μmol/g catalyst). The carbon was determined in the form of CO_2 by treating the catalyst with O_2 pulses at 923 K. The O_2 consumption was, however, much higher (<1.0 μmol/g catalyst) than that required for the CO_2 formation. Extension of the measurement to 3 h, the amount of carbon and the O_2 consumption remained practically the same. Note that the color of the catalyst remained white during the catalytic reaction (the reduced sample is dark blue). XPS analysis of these samples showed only slight changes. The binding energy of Mo $3d_{5/2}$ was about 0.2 eV lower (at 232.2 eV) than in the case of the unused sample. The deconvolution of the spectra shows that the sample used in the oxidation of CH_4 contains 13% of Mo^{5+}. We observed the same feature for other catalyst samples.

The Raman spectrum of the used catalyst was practically the same as that of the unused sample. When the catalyst was contacted only with CH_4 at 923 K we observed only very weak peaks; the spectrum was not interpretable.

4. DISCUSSION

Before analyzing the data obtained in this study we survey the characteristics of the reactions of methane of Mo-based catalysts.

4.1. Direction of CH_4 Reaction on Mo-Based Catalyst

An interesting feature of the silica-supported MoO_3 and K_2MoO_4 catalyst is that, depending on the reaction

conditions, the reaction of CH_4 proceeds in different directions. In addition to complete oxidation we may distinguish routes yielding formaldehyde (2–21), methanol (1, 19, 21), C_2 (32), and aromatic compounds (22–26). In order to establish the important factors which may govern the reaction pathways of the CH_4 transformation, it is useful to summarize the reaction conditions under which the above compounds are formed.

Methanol formation was observed at lower temperature, 753–850 K, in the presence of water and using an excess of N_2O as oxidant. It was concluded that the O^- ion is responsible for the activation of methane and for the formation of CH_3 radicals, which react with Mo^{6+}–O^{2-} to yield methoxy ions. These ions may either decompose to HCHO and OH^- ions, or they may combine with water to give methanol (19).

As shown in this and cited works (2–21), the formation of formaldehyde occurred at higher temperature, when a large excess of CH_4 was applied and O_2 was used as oxidant.

The oxidative coupling of CH_4 to give C_2H_6 and C_2H_4 proceeds above 950 K (32). In this case the CH_4/O_2 ratio was below 2, unsupported K_2MoO_4 was used, and lower space velocity was applied.

In the absence of gaseous oxygen, methane is transformed into benzene around 973 K (22–26). Other products identified are C_2H_4, C_2H_6, and C_3H_8. The selectivity to benzene (taking into account the C-containing gaseous products) was 80–85% on MoO_3/ZSM-5, 60–65% on MoO_3/SiO_2, and 60–70% on K_2MoO_4/ZSM-5 (24–26). From the detailed examination of the catalysts it appeared that the formation of benzene and C_2 compounds was preceded by the transformation of MoO_3 to Mo_2C (25, 26). This compound exhibits a moderate activity to produce CH_3 and CH_2 species from CH_4, but less activity toward their complete decomposition. As a result, the probability of the couplings of CH_3 and CH_2 to yield C_2H_6 and C_2H_4 was greatly enhanced (26). The oligomerization and aromatization of ethylene proceeded on the acidic sites of the supports.

4.2. *Some Properties of Supported K_2MoO_4*

As supported MoO_3 is an important catalyst, detailed physicochemical measurements have been performed for its surface characterization (6–8, 14, 18, 34, 35). Less information is available for supported and unsupported alkali metal molybdates (29). We found that the Raman frequencies of unsupported K_2MoO_4 agree well with those determined before (34). During the impregnation of the supports in the basic solution (pH 11) of K_2MoO_4, we observed a significant decrease in the pH value, when we used silica. In the Raman spectrum of the dried and calcined sample new Raman shifts appeared at 931 and 908 cm^{-1}, which become weaker when the pH of the suspension was increased to 11. These Raman shifts were missing from the spectrum of unsupported K_2MoO_4, but they were the dominant spectral feature for $K_2Mo_2O_7$. This strongly suggests the occurrence of polymerization of MoO_4^{2-} ions during the impregnation procedure and the formation of $Mo_2O_7^{2-}$ ions. As we observed weak peaks at 931 and 908 cm^{-1} in the Raman spectrum of the K_2MoO_4/SiO_2(II) sample, even when the pH value was kept at the value of 11 during the impregnation, we may conclude that the dimerization of K_2MoO_4 is promoted by the acidic sites of the SiO_2 surface. The ratio of the mono- and dimolybdates probably depends on the number of the surface acidic sites.

Note that the 931 and 908 cm^{-1} peaks were practically absent in the spectrum of the K_2MoO_4/TiO_2 surface, where only a slight decrease in the pH value of the K_2MoO_4/TiO_2 slurry was registered.

The XP spectra of K_2MoO_4 show that the binding energy of Mo $3d_{5/2}$ appeared at a lower value than for the bulk MoO_3. When the K_2MoO_4 is supported on different oxides, the binding energies of Mo $3d_{5/2}$ and K $2p_{3/2}$ is shifted to higher values (Table 1).

As the detection depth of the XPS technique is limited to less than ca. 2–4 nm from the surface, the atomic ratios determined by XPS represent information on the surface layer, or on just a few layers of the samples. Therefore the ratios of the peak areas for different samples can be regarded as the surface atomic ratios. Table 1 contains these ratios of the Mo $3d$ doublet for different supported K_2MoO_4 samples related to unit area of silica-supported samples. The data suggest that the amount of surface Mo atoms on K_2MoO_4/TiO_2 is more than 9 times higher than that on the K_2MoO_4/SiO_2. Note that with the increase of the amount of surface Mo atoms the binding energies of Mo $3d_{5/2}$ and K $2p_{3/2}$ exhibit a maximum.

The temperature-programmed reduction profile of K_2MoO_4 is similar to that of MoO_3/SiO_2. The reduction proceeds in practically the same temperature range, but the onset temperature of the reduction is lower by about 150 K, and the main peak is preceded by a small peak in the case of K_2MoO_4/SiO_2. The extent of the reduction was the same in both cases (29).

4.3. *Catalytic Performance of K_2MoO_4*

As mentioned in the Introduction, supported K_2MoO_4 proved to be an effective and selective catalyst in the oxidative dehydrogenation of ethane with N_2O (28, 29). The advantage of K_2MoO_4 compared to MoO_3 with or without alkali additives was the higher and more stable activity and the higher selectivity to acetaldehyde (28).

Supported K_2MoO_4 was found to be an active catalyst in the oxidation of methane, too. Its catalytic performance strongly depended on its composition and also on the nature of the support. From the comparison of the activity of different catalysts prepared in the same way, we can conclude that the highest initial CH_4 conversion was observed for MgO-, followed by Al_2O_3-, SiO_2-, ZSM-5-, and TiO_2-supported K_2MoO_4. If we relate the rate of CH_4

consumption to the number of surface Mo atoms, judged from the analysis of XPS measurements, the highest value is obtained for K_2MoO_4/MgO, followed by K_2MoO_4/SiO_2, K_2MoO_4/Al_2O_3, K_2MoO_4/ZSM-5, and K_2MoO_4/TiO_2.

With regard to the formation of formaldehyde, the silica-containing support was found to be the most effective. Highest formaldehyde selectivity, 32–33%, was measured for K_2MoO_4/SiO_2 containing a larger amount of $Mo_2O_7^{2-}$ species. This is a steady state value obtained at 923 K for a conversion of 1.3%. At lower temperature, where the CH_4 conversion was also lower, the selectivity to formaldehyde attained a value of 50% (Fig. 6B). Similar data were obtained for K_2MoO_4/ZSM-5 prepared in the same way. The use of titania support led to a decrease in the selectivity to HCHO. On K_2MoO_4/Al_2O_3, the HCHO selectivity at steady state was only 3.7% and on K_2MoO_4/MgO, formaldehyde was not detected in the reaction products. In these cases the total oxidation of methane was the dominant process.

If we compare these data with those obtained for silica-supported MoO_3 under the same conditions, we can say that the HCHO selectivity is practically the same, but the conversion of methane is somewhat higher in the latter case. The activation energies of the formation of products on K_2MoO_4/SiO_2 were practically the same as those found by Spencer and Pereira (3) on MoO_3/SiO_2, with the exception of the value for HCHO formation, which is lower in the present case.

Comparing our results for K_2MoO_4/SiO_2 with those obtained for potassium-promoted MoO_3/SiO_2 (3, 18), we can state that the reaction takes place in the same temperature range with almost the same selectivity. C_2 formation, however, was not reported on K-promoted catalysts.

4.4. Possible Mechanism of the Methane Oxidation

In our previous studies (28, 29) we assumed that the mechanism of ethane oxidation on SiO_2-supported alkali metal molybdates can be described in terms of selective cycles which produce C_2H_4 and CH_3CHO and in terms of a nonselective cycle which yields carbon dioxide. In this case we can also presume that there is a selective route and a nonselective cycle for the methane conversion.

There is a general agreement that the methane activation involves the removal of a hydrogen atom by surface O to give adsorbed methyl groups. Based on spectroscopic evidence, Liu *et al.* (19) assumed that the reaction is initiated by the formation of O^- at the Mo^{VI} sites of the surface. These ions were responsible for the H abstraction from CH_4 to form methyl radicals which react rapidly with the surface to form methoxide. This complex may then decompose to HCHO or react with water to form CH_3OH.

Smith and Ozkan (14) proposed that terminal oxygen (Mo=O) located on the side planes of the crystal promotes the formaldehyde production, while bridging oxygen (Mo–O–Mo) accelerates the deep oxidation of methane. Suzuki *et al.* (16) suggested that the active species for formaldehyde formation are the well dispersed molybdenum oxide clusters on SiO_2. Kasztelan and Moffat (6, 7) found that 12-molybdosilicic acid ($H_4SiMo_{12}O_{40}$) is formed on the MoO_3/SiO_2 catalysts and that this was the active center for the oxidation of methane (8).

Regarding the oxygen species involved in the oxidation process we point out that the O^{2-} ions of K_2MoO_4 react easily with methane under the experimental conditions as indicated by the formation of CO_2 and H_2O following the interaction of methane with K_2MoO_4 in the absence of gaseous oxygen (25). In this case, however, HCHO was not identified in the reaction products. This suggests that not the lattice O^{2-}, but more probably the adsorbed oxygen ion is responsible for the selective route of methane oxidation on K_2MoO_4, i.e., in the activation of CH_4 and in the formation of methoxy species. Accordingly we propose the following steps for the selective oxidation

$$CH_4(g) + O^-(s) = CH_3(s) + OH^-$$
$$CH_3(s) + O^-(s) = CH_3{-}O^-(s).$$

Methoxy species react further with OH^- ion to give formaldehyde

$$2\,Mo^{6+} + CH_3{-}O^- + OH^- \rightarrow HCHO + 2Mo^{5+} + H_2O.$$

This reaction scheme for the formation of HCHO is supported by the results of Sun *et al.* (13). They used a double-layered catalyst bed of Sr/La_2O_3 (which produces the CH_3 radicals) followed by MoO_3/SiO_2 and found that the formaldehyde yield is significantly higher compared to a single bed catalyst containing only silica-supported MoO_3. The fact that we detected the formation of CH_3OH in a small amount may suggest that the same elementary steps are responsible for the formation of HCHO on K_2MoO_4/SiO_2 catalyst, too.

The results shown in Fig. 6 suggest that a fraction of the HCHO formed can decompose and/or oxidize first to CO and then to CO_2. Corresponding to the nature of secondary reactions, an increase in the contact time decreased the HCHO selectivity but enhanced the CO selectivity. If we accept that the main part of CO formed in this way we can state that the selective route of the reaction produces nearly the same amount of products on the two silica-supported molybdates (Table 3). The different decomposition or reaction rates of HCHO to CO can result in the differences of the selectivities of HCHO and CO formation. The structure of the molybdenum compounds very probably plays an important role in the determination of the reaction pathways as on the K_2MoO_4/SiO_2 containing a larger amount of $K_2Mo_2O_7$ (Table 3); the rate of HCHO formation significantly increased while that of CO evolution decreased. The fact that the formation of HCHO was much less on titania-,

and alumina-, and was completely missing on magnesia-supported catalyst suggests that in addition to the structure of molybdenum compounds their acid–base properties also affect the selectivity of the catalysts.

In addition to the above reactions, we may assume the dimerization of the methyl groups to give C_2H_6

$$2\,CH_3 = C_2H_6$$

and/or the decomposition of CH_3 species to hydrogen and carbon

$$CH_3 = C + 1.5\,H_2.$$

However, we found no or only an extremely small amount of surface carbon after the catalytic run, so this route of CH_3 reaction in the presence of oxygen is negligible. The products of total oxidation, CO_2 and H_2O, could be the result of the direct oxidation of CH_3 and/or HCHO.

4.5. Reaction of Methane at Very Low Oxygen Pressure

A separate discussion is required for the results obtained at very low oxygen contents. This part of the study was initiated by our recent observation that methane is transformed into benzene on K_2MoO_4/ZSM-5 catalyst in the absence of gaseous oxygen (25). This route of the methane conversion was markedly diminished by adding only 0.1% of O_2 to methane, and was completely poisoned in the presence of 1% of O_2. Accordingly, this small amount of oxygen is sufficient to prevent the reduction of Mo^{6+} and the formation of a new compound, Mo_2C, assumed to be important for the conversion of methane to benzene (26). At the same time, due to the consumption of O^{2-} ions, the extent of the total oxidation is also decreased. Due to the lack of adsorbed O (0.1% O_2 content) HCHO did not form or formed only to a small extent (1% O_2 content).

Finally, it should be mentioned that the partial oxidation of methane is also being investigated on other alkali metal molybdates. All are active catalysts for this oxidation. The conversion of CH_4 increased from Li to Cs, while the selectivity to HCHO production has a maximum for K_2MoO_4 (37).

ACKNOWLEDGMENTS

Financial support of this work by OTKA (Contract T 014921) is gratefully acknowledged. The authors express their thanks to Dr. O. Berkesi for carrying out the Raman spectra, to A. Oszkó for his assistance in the XPS measurements, and to the Phare-Accord program (H-9112-0152) for financial support for the Raman spectrometer.

REFERENCES

1. Foster, N. R., *Appl. Catal.* **19**, 1 (1985).
2. Pitchai, R., and Klier, K., *Catal. Rev.-Sci. Eng.* **28**, 13 (1986).
3. Spencer, N. D., and Pereira, C. J., *A.I.CheE.J.* **33**, 1808 (1987).
4. Spencer, N. D., *J. Catal.* **109**, 187 (1988).
5. Otsuka, K., and Hatano, M., *J. Catal.* **108**, 252 (1987).
6. Kasztelan, S., and Moffat, J. B., *J. Catal.* **106**, 512 (1987).
7. Kasztelan, S., and Moffat, J. B., *J. Catal.* **112**, 54 (1988).
8. Kasztelan, S., Payen, E., and Moffat, J. B., *J. Catal.* **112**, 320 (1988).
9. Spencer, N. D., Pereira, C. J., and Grasselli, R. K., *J. Catal.* **126**, 546 (1990).
10. Banares, M. A., Rodriguez-Ramos, I., Guerrero-Ruiz, A., and Fierro, J. L. G., *Catal. Lett.* **17**, 205 (1993).
11. Weng, T., and Wolf, E. E., *Appl. Catal.* **96**, 383 (1993).
12. Barbaux, Y., Elamrani, A. R., Payen, E., Gengembre, L., Bonnelle, J. P., and Grzybowska, B., *Appl. Catal.* **44**, 117 (1988).
13. Sun, Q., Di Cosimo, J. I., Herman, R. G., Klier, K., and Bhasin, M., *Catal. Lett.* **15**, 371 (1992).
14. Smith, M. R., and Ozkan, U. S., *J. Catal.* **141**, 124 (1993).
15. Irusta, S., Lombardo, E. A., and Miro, E. E., *Catal. Lett.* **29**, 339 (1994).
16. Suzuki, K., Hayakawa, T., Shimizu, M., and Takehira, K., *Catal. Lett.* **30**, 159 (1995).
17. Arena, F., Frusteri, F., Parmaliana, A., and Giordano, N., *Appl. Catal. A: General* **125**, 39 (1995).
18. Banares, M. A., Spencer, N. D., Jones, M. D., and Wachs, I. E., *J. Catal.* **146**, 204 (1994).
19. Liu, H. F., Liu, R. S., Liew, K. Y., Johnson, R. E., and Lunsford, J. H., *J. Am. Chem. Soc.* **106**, 4117 (1984); Lunsford, J. H., "Proc. Int. Congr. Catal., 10th, Budapest, 1992" (L. Guczi, F. Solymosi, and P. Tétényi, Eds.), p. 103, Akadémiai Kiadó, Budapest, 1993.
20. Liu, R. S., Iwamoto, J., and Lunsford, J. H., *J. Chem. Soc. Chem. Commun.* **78** (1982).
21. Khan, M. M., and Somorjai, G. A., *J. Catal.* **91**, 263 (1985).
22. Wang, L., Huang, L., Xie, M., and Xu, G., *Catal. Lett.* **21**, 35 (1993).
23. Xu, Z., Liu, S., Wang, L., Xie, M., and Guo, X., *Catal. Lett.* **30**, 135 (1995).
24. Solymosi, F., Erdőhelyi, A., and Szőke, A., *Catal. Lett.* **32**, 43 (1995).
25. Szőke, A., and Solymosi, F., *Appl. Catal. A: General* **142**, 361 (1996).
26. Solymosi, F., Szőke, A., and Cserényi, J., *J. Catal.*, in press.
27. Mendelovici, L., and Lunsford, J. H., *J. Catal.* **94**, 37 (1985).
28. Erdőhelyi, A., Máté, F., and Solymosi, F., *Catal. Lett.* **8**, 229 (1991).
29. Erdőhelyi, A., Máté, F., and Solymosi, F., *J. Catal.* **135**, 563 (1992).
30. Erdőhelyi, A., and Solymosi, F., *J. Catal.* **123**, 31 (1990). Erdőhelyi, A., and Solymosi, F., *Appl. Catal.* **39**, L11 (1988). Erdőhelyi, A., and Solymosi, F., *J. Catal.* **129**, 497 (1991).
31. Kung, H. H., *Adv. Catal. Relat. Subj.* (D. D. Eley, H. Pines, and W. O. Haag, Eds.), **40**, 1 (1994).
32. Kiwi, J., Thampi, K. R., and Grätzel, M., *J. Chem. Soc. Chem. Commun.* 1690 (1990).
33. Romijn, G., *Z. Anal. Chem.* **39**, 60 (1900).
34. Kim, D. S., Segawa, K., Soeya, T., and Wachs, I. E., *J. Catal.* **136**, 539 (1992).
35. Rocchiccioli-Deltcheff, C., Amirouche, M., Che, M., Tatibouët, J.-M., and Fournier, M., *J. Catal.* **125**, 292 (1990).
36. von Becher, H. J., *Z. Anorg. Allg. Chem.* **474**, 63 (1981).
37. Fodor, K., Oszkó, A., Erdőhelyi, A., and Solymosi, F., to be published.